

PROCEEDINGS OF SPIE

***Next Generation (Nano) Photonic  
and Cell Technologies for Solar  
Energy Conversion II***

**Loucas Tsakalacos**

*Editor*

**21–23 August 2011**

**San Diego, California, United States**

*Sponsored and Published by*  
SPIE

**Volume 8111**

Proceedings of SPIE, 0277-786X, v. 8111

SPIE is an international society advancing an interdisciplinary approach to the science and application of light.

# Silicon nanowire solar cells with a-Si hetero-junction showing 7.3% efficiency

Fritz Falk<sup>1</sup>, Guobin Jia<sup>1</sup>, Gudrun Andrä<sup>1</sup>, Ingo Sill<sup>1</sup>, Nikolay Petkov<sup>2</sup>

<sup>1</sup> Institute of Photonic Technology, Albert-Einstein-Str. 9, 07745 Jena, Germany

<sup>2</sup> Tyndall National Institute, Cork, Ireland

## ABSTRACT

Core-shell silicon nanowire (SiNW) solar cells with an a-Si heterojunction were prepared on SiNW arrays, which were etched into n-type silicon wafers or into n-doped multicrystalline silicon thin films on glass substrates. A stack of intrinsic and p-doped hydrogenated a-Si was deposited as a shell around the SiNWs by PECVD, acting as a hetero-emitter of the solar cells. Finally a TCO layer consisting of aluminum doped zinc oxide was deposited on top of the a-Si by atomic layer deposition. In a mesa-structured solar cell (area 7 mm<sup>2</sup>) an open circuit voltage of 476 mV and an efficiency of 7.3% were achieved under AM 1.5 illumination. Electron beam induced current measurements show clear evidence that most of the photo-current comes from the thin SiNW layer.

**Keywords:** Solar cells, silicon, nanowires, hetero-junction

## 1. INTRODUCTION

Solar cells based on silicon nanowires have received growing interest during the last few years<sup>1-8</sup>. As compared to classical silicon wafer cells they need at least two orders of magnitude less high purity silicon. Competing thin film cells based on hydrogenated amorphous silicon show a rather low efficiency of 7% to 8% in production. a-Si/ $\mu$ c-Si tandem cells show 10% to 11% efficiency but are rather expensive in production since they need a silicon thickness of about 2  $\mu$ m and must be deposited by PECVD at a low rate (in the 10 nm/min range), which adds to the production costs. Therefore, these types of thin film solar cells are struggling hard against the silicon wafer cells. The cells with the best efficiency/cost ratio are CdTe thin films cells with about 11% efficiency in production. However, there are environmental concerns due to the cadmium present in these cells. A further competitor is the CIGS (copper-indium-gallium-selenide) thin film cell with similar efficiency. There, however, the availability of indium is an issue. As an alternative, crystalline silicon thin film cells are under consideration. Since crystalline silicon is an indirect semiconductor with a band gap of 1.1 eV, its absorption of the solar spectrum is somewhat low for a thin film cell. Consequently, either rather thick films are needed, which leads to increased costs, particularly if PECVD is used for deposition, or a perfect light trapping scheme has to be implemented. The latter is the basic idea of silicon nanowire cells. Light entering a carpet of silicon nanowires (diameter several 10 to 100 nm, length in the  $\mu$ m range) is strongly scattered. So, the light does not just pass straight through the film but takes an irregular way leading to a much stronger absorption as compared to a film of the thickness of the length of the nanowires. Silicon nanowires form a perfect light trapping structure<sup>9,10</sup> which appreciably enhanced light absorption.

For the preparation of silicon nanowires, two methods are well known. In a bottom up method the nanowires are grown by VLS growth<sup>11</sup> (vapor liquid solid) via thermal CVD. Typically the growth is catalyzed by gold nanotemplates of the size of the desired nanowire diameter. As templates one can use commercially available gold colloids with a rather narrow diameter distribution. The other possibility is to prepare the gold nanodroplets from a thin (about 1 nm) gold film on a silicon substrate by tempering above the eutectic temperature of the Au-Si system of 370°C. During tempering a very thin liquid film forms which disintegrates into the desired droplets. The nanowires are then grown by thermal CVD from silane (SiH<sub>4</sub>) at about 500°C. Silane is rather stable at this temperature and just decomposes catalytically at the gold droplets. The droplets get supersaturated by silicon which precipitates at the area where the droplet is in contact with the silicon substrate so that no nucleation is needed. As a consequence, a nanowire grows beneath each gold droplet with a diameter similar to that of the droplet. Finally the droplet rests on top of the nanowire and afterwards can be removed by some etching process, e.g. by aqua regia. However, some gold is incorporated into the nanowire<sup>12-14</sup> (dissolved or as nanoclusters at the surface). There is some discussion in the literature concerning the detrimental influence of these gold

remnants for the photovoltaic properties of the nanowires by reducing the lifetime of minority charge carriers<sup>15</sup>. Nevertheless, the crystal quality of the nanowires is rather perfect, that is they are single crystalline, sometimes with a twin boundary<sup>16</sup>.

Alternatively, there exists a top down nanowire preparation method by etching. By a rather simple method<sup>17</sup> single crystalline or multicrystalline silicon can be etched in a self-organized way to form nanowires. This method is used in our approach and is presented in Section 3. This method, too, results in single crystalline silicon nanowires, even if prepared from a multicrystalline substrate.

Both methods work on silicon wafers (single or polycrystalline) as well as on multicrystalline silicon thin films. It is quite clear that silicon wafers are a perfect substrate for developing the preparation methods. However, for solar cell production wafers as a substrate do not make too much sense, since the nanowire cell on top of the wafer will hardly show a higher efficiency than a wafer cell. The nanowire preparation would just introduce some additional production steps with the result of even decreasing the efficiency. In a production environment, nanowires probably are useful only if prepared on a cheaper substrate, e.g. a silicon thin film on glass.

## 2. NANOWIRE SOLAR CELL CONCEPTS

There are two concepts of nanowire solar cells, with axial or with radial pn-junction<sup>1</sup>. Both have their advantages and disadvantages, so that it is not absolutely clear which one should lead to better solar cells. In the axial case the doping changes along the length of the nanowires (Fig. 1 left). The advantage in this case is that the photocurrent generated within the nanowire passes through the small cross section area leading to a high photocurrent density  $j_{ph}$  at the p-n junction. According to the equation for the open circuit voltage

$$V_{oc} = \frac{kT}{e} \ln \frac{j_{ph}}{j_s} \quad (1)$$

( $j_s$  is the saturation current density of the p-n junction) the open circuit voltage should be enhanced. The disadvantage is that the distance between light induced charge carrier generation and their separation at the p-n junction is large, namely about half the nanowire length. Therefore, the quality of the nanowire bulk is extremely important to reduce bulk recombination. Moreover, there is a huge surface area of the nanowires where surface recombination may occur. Therefore, a perfect surface passivation of the nanowires is crucial. In the case of a radial p-n junction (Fig. 1 right) the nanowire is covered by an oppositely doped shell so that the complete outer surface forms the p-n junction. In this case the area of the p-n junction is large, and the photocurrent density is low, so that according to eq. 1 the open circuit voltage should be reduced. On the other hand, the distance between light induced charge carrier generation and separation at the p-n junction is short, namely less than half the nanowire diameter, so that the quality of the nanowire bulk is not as important. Moreover, the passivation at the outer surface of the nanowire shell acting as emitter is not as crucial. Which of the concepts leads to better solar cells depends on the quality of the nanowire bulk and of the quality of the surface passivation and hardly can be predicted presently.

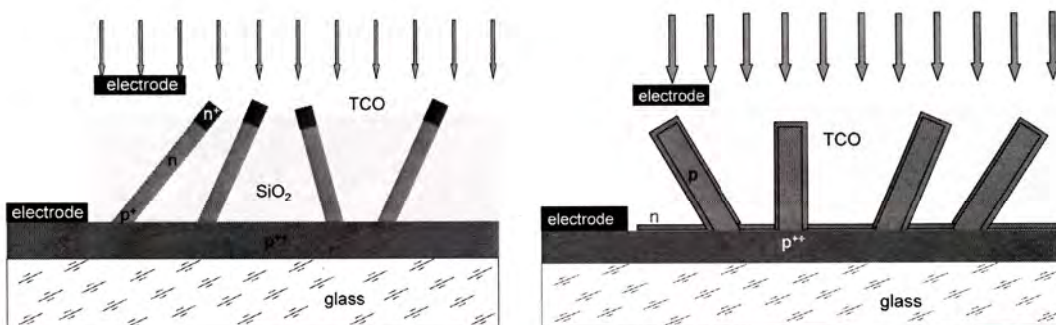


Fig. 1. Concept of silicon nanowire solar cells with axial (left) and radial (right) p-n junction

In this paper nanowire solar cells with radial p-n junction are investigated. The concept of the cells is as follows. The nanowires are etched into a n-type silicon wafer or into a silicon thin film. The emitter consists of p-doped hydrogenated amorphous silicon deposited by classical PECVD, so that a hetero-junction forms. As front contact aluminum doped ZnO is deposited as a transparent conductive oxide. Since silicon wafer cells with a-Si heteroemitter<sup>18-20</sup> are the wafer cells with the highest efficiency in production, this concept has been chosen for our nanowire solar cells as well.

### 3. EXPERIMENTAL

The nanowires were prepared by wet chemical etching according to a procedure described by Peng<sup>17</sup>. As substrates we used n-doped silicon wafers ( $1 \times 10^{15} \text{ cm}^{-3}$  phosphorus) or n-doped multicrystalline silicon thin films, which were prepared by the LLC (layered laser crystallization) process<sup>21</sup>. In this process first a thin hydrogen free amorphous silicon layer (100 to 200 nm) is deposited by electron beam evaporation. This layer is crystallized by scanning the beam of a diode laser (line focus  $12 \times 0.1 \text{ mm}$ , up to  $25 \text{ kW/cm}^2$ , scanning speed  $5 \text{ cm/s}$ ). The laser melts the silicon film for several ms, which then crystallizes to grains with sizes in the  $100 \text{ }\mu\text{m}$  range. This multicrystalline layer is used as a seed for further epitaxial thickening. After removal of the natural oxide layer the seed is transferred into the electron beam evaporator. During a-Si deposition (rate e.g.  $500 \text{ nm/min}$ ) the growing film is repeatedly irradiated by the beam of an excimer laser (248 nm wavelength, 25 ns pulse duration, about  $550 \text{ J/cm}^2$  fluence) which is fed through a window of the deposition chamber. The laser pulses are repeated whenever about  $50 \text{ nm}$  of a-Si are newly deposited. The a-Si film and a bit of the crystalline Si film beneath are melted for about  $100 \text{ ns}$  to epitaxially crystallize on the crystalline Si. The process is continued until the desired film thickness (e.g.  $1.5 \text{ }\mu\text{m}$ ) is reached. To irradiate the whole area of deposition (in our case  $10 \times 10 \text{ cm}^2$ ) the laser beam is scanned over the substrate by a scanning mirror outside the deposition chamber. Crystallization does not take any time additional to high rate deposition.

In both cases, wafer and thin film, the substrates for nanowire etching first were cleaned by acetone and 2-propanol, and then at  $80 \text{ }^\circ\text{C}$  for about 10 minutes by a solution of  $\text{H}_2\text{SO}_4$  (97%) and  $\text{H}_2\text{O}_2$  (30%) (1:1 by volume) to remove any organic and inorganic contaminations from the surface. The cleaned substrate was mounted in an etching cell which allows only the upper side to get in contact with the etching solution. For nanowire etching a mixture of  $10 \text{ ml AgNO}_3$  (0.02 M) and  $10 \text{ ml HF}$  (5 M) at room temperature was applied for 30 minutes. Then the sample was rinsed thoroughly with deionized water. In the etchant nanoparticles of silver form which catalyze the self-organized etching of channels into the silicon substrate so that silicon nanowires remain. After etching there are silver dendrites at the outer surface and silver nanoparticles in the holes between the nanowires. Before further solar cell preparation the silver particles have to be removed carefully to avoid shunting of the cells. The cleaning procedure begins with a 3 min. dip in concentrated  $\text{HNO}_3$  (65%) to remove the large amount of silver dendrites on the sample surface. The sample then is rinsed in deionized water for several times. After that  $10 \text{ ml NH}_4\text{OH}$  (4.6%) together with  $5 \text{ ml}$  2-propanol is added to the etching cell. Air is bubbled through the mixture for 25 minutes. The oxygen in the air oxidizes the Ag particles to Ag ions, and  $\text{NH}_4\text{OH}$  reacts with the Ag ions to form a soluble complex. 2-propanol serves as a surfactant to reduce the surface tension allowing the etchant to penetrate into the holes between the nanowires to remove the silver particles at the bottom of the nanowires. It should be noted that prolonged treatment in  $\text{NH}_4\text{OH}$  solution could result in removal of the nanowire layer, as silicon dissolves in alkaline solutions<sup>22-24</sup>. In a further silver removal step the sample was treated by a neutral  $\text{Na}_2\text{S}_2\text{O}_3$  (0.1 M):2-propanol solution for 20 min. The 2-propanol again acts as a surfactant. Silver forms a soluble complex with the thiosulfate ion  $\text{S}_2\text{O}_3^{2-}$ . After the cleaning, the sample was dipped into a HF (2%):2-propanol solution for 8 minutes to remove the oxide layer on the nanowire surface. The 2-propanol again serves as a surfactant so that the etchant can penetrate into the nanowire array to remove the oxide around the NWs completely. It is crucial in this step to use a surfactant, because when the oxide on the tips of the nanowires is removed, the surface turns from hydrophilic into hydrophobic. Therefore, without surfactant HF will not penetrate to the bottom of the SiNW arrays.

After rinsing in deionized water, the sample was immediately placed into the PECVD chamber to deposit the a-Si layer at  $225 \text{ }^\circ\text{C}$ . Thin intrinsic a-Si (20 seconds at a silane flow rate of  $2 \text{ sccm}$ , chamber pressure of  $0.5 \text{ mbar}$ ) was deposited prior to highly p-doped a-Si (2 min. at a silane flow rate of  $2 \text{ sccm}$  and diborane of  $1 \text{ sccm}$  (2% diluted in He), chamber pressure  $0.5 \text{ mbar}$ ). Intrinsic a-Si is very effective in reducing the surface recombination at the interface of a-Si/c-Si<sup>18,25,26</sup>. As a transparent conductive oxide (TCO), about  $200 \text{ nm}$  polycrystalline aluminum doped zinc oxide (AZO) was deposited on top of the a-Si layer at a substrate temperature of  $225 \text{ }^\circ\text{C}$  by atomic layer deposition (ALD).

The samples were mesa-etched and the contact areas of the solar cells were determined by a microscope. Finally, in case of wafers as a substrate, the ohmic back side contact was made by rubbing InGa alloy on the rear side of the wafer. In case of silicon thin films as a substrate, the highly doped seed layer was used as contact.

For structural characterization the samples, in different preparation stages, were investigated by a JEOL field emission scanning electron microscope (SEM) and by transmission electron microscopy (TEM). For TEM cross-sectional analysis the samples were prepared by in-situ lift out using FEI's Helios NanoLab systems equipped with an Omiprobe micro-manipulator. Special care was taken by final polishing of the lamella because of the heterogeneous nature of the specimens. TEM images were taken by a JEOL 2100 HRTEM, operated at 200 kV. Optical characterization of the nanowires etched into a silicon thin film was performed in an UV-Vis spectrometer using an integrating sphere. In this way, reflection  $R$  and transmission  $T$  were measured and absorption  $A$  was determined according to  $A=1-T-R$ . An integrating sphere is necessary since even by the naked eye one immediately observes that there is nearly no specular reflection but only small omnidirectional reflection. I-V-curves were measured in the dark and under AM1.5 illumination by a cw sun simulator. To make sure that most of the photocurrent really does come from the nanowires and not from the silicon substrate, EBIC (electron beam induced current) measurements were performed on the surface of the sample as well as on a cross section.

#### 4. RESULTS

After the different preparation steps the samples were characterized by SEM and by TEM. Fig. 2 shows a TEM micrograph of a nanowire from a processed solar cell showing the nanowire core (SiNW), the amorphous shell of the emitter, and the TCO. The nanowire was imaged after tilting the thin foil along the [110] zone axis. Hence the interface of the {110} set of planes with the aSi layer is visualized. The total thickness of the intrinsic and p-type a-Si is about 4 nm (Fig. 2 right). Polycrystalline AZO fills most of the space between the nanowires. Such a structure provides a low resistance front contact.

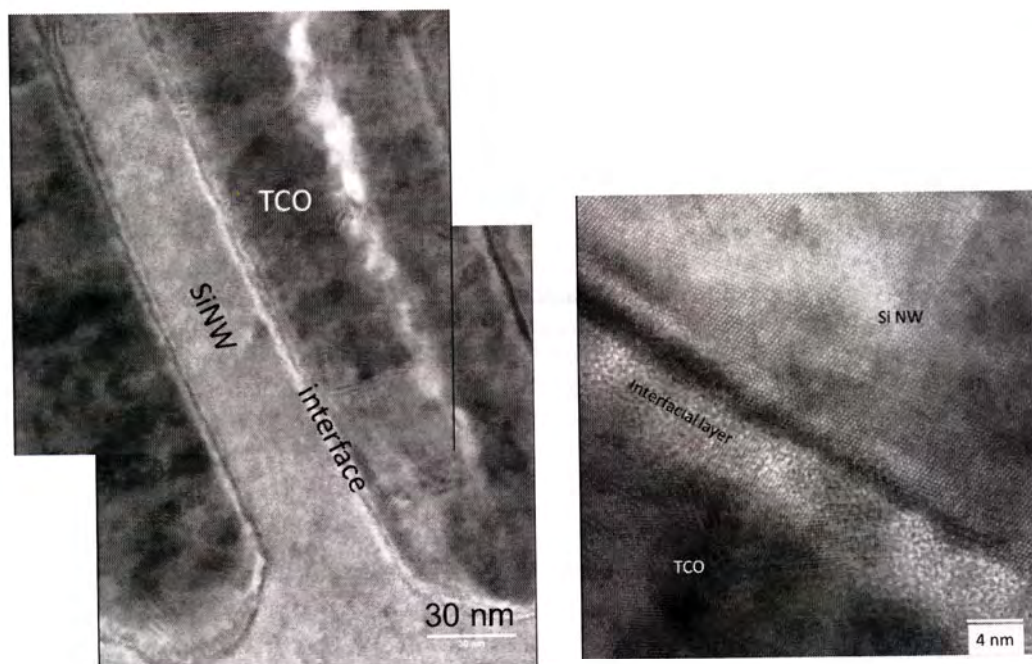


Fig. 2. TEM image of a single nanowire of a processed nanowire solar cell (left) and HRTEM image of a region including the a-Si shell

Fig. 3 shows the reflection, transmission, and absorption of a 1.5  $\mu\text{m}$  thick crystalline silicon thin film on glass prior and after etching of nanowires. Obviously, the reflection of the nanowire sample in the visible wavelength range is much

lower as that of the original silicon thin film, namely in the 5% range. The average transmission of both is similar with the difference, that in the virgin film oscillations due to interference effects occur. Consequently, the absorption of the nanowire sample is much higher, in the 90% range up to 550 nm, that is about twice that of the virgin silicon film. This demonstrates the light trapping effect of the nanowire carpet.

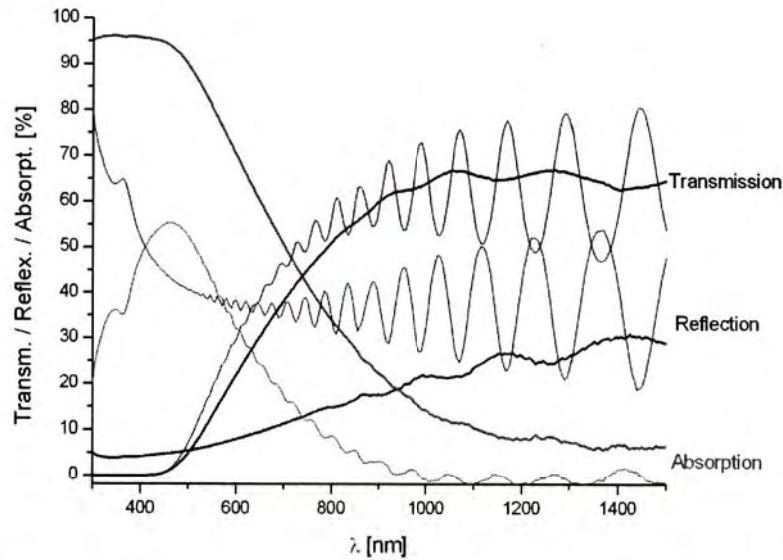


Fig.3. Reflection, transmission, and absorption of a 1.5  $\mu\text{m}$  thick crystalline silicon thin film in the virgin state (thin lines) and after nanowire etching (bold lines)

In Fig. 4 I-V curves from a 7 mm<sup>2</sup> nanowire cell on a silicon wafer are shown as taken in the dark and under AM1.5 illumination. The dark curve shows an ideal diode characteristic. No shunting at reverse bias was observed for all the cells. This indicates that the metallic impurities on the surface were effectively removed by the cleaning procedure. Under AM1.5 illumination the sample showed the following solar cell parameters:  $V_{OC}$  476 mV,  $j_{SC}$  27.0 mA/cm<sup>2</sup>, 7.3% efficiency. EBIC investigations demonstrate that the current is generated in the nanowire carpet and not in the substrate<sup>27</sup>.

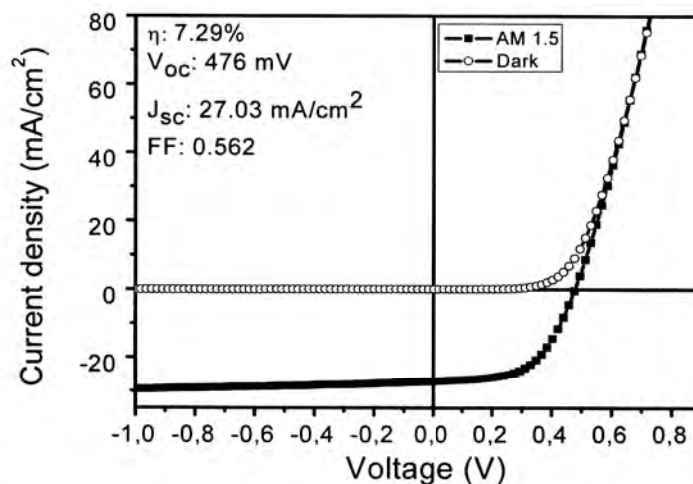


Fig. 4. I-V characteristics of a nanowire solar cell on a silicon wafer with an area of 7 mm<sup>2</sup> in the dark and under AM 1.5 illumination.

In Fig. 5 an I-V-curve of a nanowire cell prepared on a 1.5  $\mu\text{m}$  thick multicrystalline silicon thin film on glass is shown. The cell was prepared on the same nanowire carpet, the optical properties of which are shown in Fig. 3. The quality of the cells prepared on silicon thin films is less than that of those prepared on wafers. The cell reached an open circuit voltage of 385 mV and an efficiency of 1.9% only. Presently it is not clear, what is the reason for the differences.

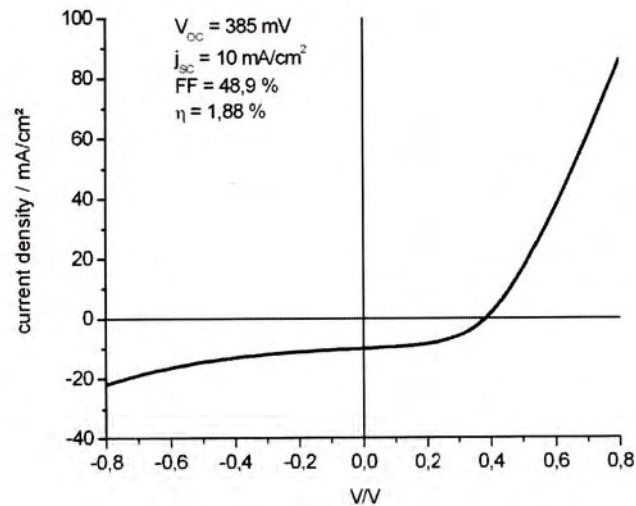


Fig. 5. I-V characteristics of a nanowire solar cell on a multicrystalline silicon thin film with an area of 4 mm<sup>2</sup> under AM 1.5 illumination.

## 5. SUMMARY

Highly efficient core-shell TCO/a-Si/Si nanowire hetero-junction solar cells have been fabricated on silicon nanowire arrays prepared cost-effectively by metal assisted wet chemical etching on silicon wafers and on silicon thin films. It was demonstrated that the nanowire carpet acts as a perfect light trapping structure. Great improvement concerning the optoelectronic properties and of the energy conversion efficiency was obtained in comparison with previous solar cells<sup>3,7</sup> based on SiNW arrays produced in a similar way. The improvement is attributed to a thorough three-step cleaning procedure removing silver particles even from the holes between nanowires. Nevertheless, metal contamination may still be a challenge to further improve the solar cell performance. A better procedure has to be found to ensure the cleaning of densely packed nanowire arrays while keeping them intact. Further optimization of the cleaning procedures, the morphology of the nanowire arrays (diameters, lengths and density), and the a-Si and TCO deposition, respectively, is in progress.

## 6. ACKNOWLEDGEMENT

The authors would like to acknowledge the financial support by the European Commission in Projects SiNAPS under contract number 257856 and NanoPV under contract 246331. The author would like to thank Prof. Martin Kittler and Winfried Seifert for their support in measuring EBIC at IHP/BTU Joint Lab, Cottbus, Germany. We also very much appreciate the SEM images taken at IPHT by Sarah Hausschild and Andy Scheffel.

## 7. REFERENCES

- [1] Kayes, B. M., Atwater, H.A. and Lewis, N.S., "Comparison of the device physics principles of planar and radial p-n junction nanorod solar cells", *J. Appl. Phys.* 97, 114302 (2005).
- [2] Yoon, H. P., Yuwen, Y. A., Kendrick, C. E., Barber, G. D., Podraza, N. J., Redwing, J. M., Mallouk, T. E., Wronski, C. R. and Mayer, T. S., "Enhanced conversion efficiencies for pillar array solar cells fabricated from crystalline silicon with short minority carrier diffusion lengths", *Appl. Phys. Lett.* 96, 213503 (2010).
- [3] Wang, X., Pey, K. L., Yip, C. H., Fitzgerald, E. A. and Antoniadis, D. A., "Vertically arrayed Si nanowire/nanorod-based core-shell p-n junction solar cells", *J. Appl. Phys.* 108, 124303 (2010).
- [4] Kempa, T. J., Tian, B., Kim, D. R., Hu, J., Zheng, X. and Lieber, C. M., "Single and tandem axial p-i-n nanowire photovoltaic devices", *Nano Lett.* 8, 3456 (2008).
- [5] Sivakov, V., Andrä, G., Gawlik, A., Berger, A., Plentz, J., Falk, F. and Christiansen, S. H., "Silicon Nanowire-Based Solar Cells on Glass: Synthesis, Optical Properties, and Cell Parameters", *Nano Lett.* 9, 1549 (2009).
- [6] Tian, B., Zheng, X., Kempa, T. J., Fang, Y., Yu, N., Yu, G., Huang, J. and Lieber, C. M., "Coaxial silicon nanowires as solar cells and nanoelectronic power sources", *Nature* 449, 885 (2007).
- [7] Garnett E. C. and Yang, P., "Silicon nanowire radial p-n junction solar cells", *J. Am. Chem. Soc.* 130, 9224 (2008).
- [8] Tsakalakos, L., Balch, J., Fronheiser, J., Korevaar, B. A., Sulima, O. and Rand, J., "Silicon nanowire solar cells", *Appl. Phys. Lett.* 91, 233117 (2007).
- [9] Garnett E. C. and Yang, P., "Light trapping in silicon nanowire solar cells", *Nano Lett.* 10, 1082 (2010).
- [10] Kanamori, Y., Sasaki, M. and Hane, K., "Broadband antireflection gratings fabricated upon silicon substrates", *Optics Letters*, 24, 1422 (1999).
- [11] Wagner R. S. and Ellis, W. C., "Vapor-liquid-solid mechanism of single crystal growth", *Appl. Phys. Lett.* 4, 89 (1964).
- [12] Allen, J. E., Hemesath, E. R., Perea, D. E., Lensch-Falk, J. L., Li, Z. Y., Yin, F., Gass, M. H., Wang, P., Bleloch, A. L., Palmer, R. E. and Lauhon, L. J., "High-resolution detection of Au catalyst atoms in Si nanowires", *Nature Nanotech.* 3, 168-173 (2008).
- [13] Bailly, A., Renault, O., Barrett, N., Zagonel, L. F., Gentile, P., Pauc, N., Dhalluin, F., Baron, T., Chabli, A., Cezar, J. C. and Brookes, N. B., "Direct quantification of gold along a single Si nanowire", *Nano Lett.* 8, 3709 (2008).
- [14] Jackson, J. B., Kapoor, D., Jun, S. G. and Miller, M. S., "Integrated silicon nanowire diodes and the effects of gold doping from the growth catalyst", *J. Appl. Phys.* 102, 054310 (2007).
- [15] Lang, D. V., Grimmeiss, H. G., Meijer E. and Jaros, M., "Complex nature of gold-related deep levels in silicon", *J. Appl. Phys.* 22, 3917 (1980).
- [16] Teo, B. K., Sun, X. H., Hung, T. F., Meng, X. M., Wong, N. B. and Lee, S. T., "Precision-cut crystalline silicon nanodots and nanorods from nanowires and direct visualization of cross sections and growth orientations of silicon nanowires", *Nano Lett.* 3, 1735 (2003).
- [17] Peng, K., Yan, Y., Gao, S. and Zhu, J., "Synthesis of large-area silicon nanowire arrays via self-assembling nanoelectrochemistry", *Adv. Mater.* 14, 1164 (2002).
- [18] Tanaka, M., Taguchi, M., Matsuyama, T., Sawada, T., Tsuda, S., Nakano, S., Hanafusa, H. and Kuwano, Y., "Development of new a-Si/c-Si heterojunction solar cells: ACJ-HIT (artificially constructed junction-heterojunction with intrinsic thin layer)", *Jpn. J. Appl. Phys.* 31, 3518 (1992).
- [19] Wang, Q., Page, M. R., Iwaniczko, E., Xu, Y., Roybal, L., Bauer, R., To, B., Yuan, H.-C., Duda, A., Hasoon, F., Yan, Y. F., Levi, D., Meier, D., Branz, H. M. and Wang, T. H., "Efficient heterojunction solar cells on p-type crystal silicon wafers", *Appl. Phys. Lett.* 96, 013507 (2010).
- [20] Mishima, T., Taguchi, M., Sakata, H. and Maruyama, E., "Development status of high-efficiency HIT solar cells", *Solar Energy Materials & Solar Cells* 95, 18 (2011).
- [21] Andrä, G., Bergmann, J., Bochmann, A., Falk, F., Gawlik, A., Ose, E., Plentz, J., Dauwe, S. and Kieliba, T., "Multicrystalline silicon thin film solar cells based on laser crystallized layers on glass", *Proc. 2006 IEEE 4th World Conf. Photovoltaic Energy Conversion*, 1564-1567 (2006).
- [22] Yan, G., Chan, P. C. H., Hsing, I. M., Sharma, R. K., Sin, J. K. O. and Wang, Y., "An improved TMAH Si-etching solution without attacking exposed aluminium", *Sensors and Actuators*, A89, 135 (2001).
- [23] Schnakenberg, U., Benecke, W. and Löchel, B., "NH<sub>4</sub>OH-based etchants for silicon micromachining", *Sensors and Actuators*, A21-A23, 1031 (1990).



- [24] Sato, K., Shikida, M., Yamashiro, T., Asaumi, K., Iriye, Y. and Yamamoto, M., "Anisotropic etching rates of single-crystal silicon for TMAH water solution as a function of crystallographic orientation", *Sensors and Actuators*, 73, 131 (1999).
- [25] Borchert, D., Grabosch, G. and Fahrner, W. R., "Preparation of (n) a-Si:H/(p) c-Si heterojunction solar cells", *Solar Energy Materials & Solar Cells* 49, 53 (1997).
- [26] Fujiwara H. and Kondo, M., "Effects of a-Si:H layer thicknesses on the performance of a-Si:H/c-Si heterojunction solar cells", *J. Appl. Phys.* 101, 054516 (2007).
- [27] Jia, G., Steglich, M., Sill, I. and Falk, F. "Highly efficient core-shell heterojunction solar cells on silicon nanowire arrays", to be published.